Potential of Surface-Enhanced Raman Spectroscopy for the Rapid Identification of *Escherichia Coli* and *Listeria Monocytogenes* Cultures on Silver Colloidal Nanoparticles

YONGLIANG LIU, YUD-REN CHEN,* XIANGWU NOU, and KUANGLIN CHAO

Department of Nutrition and Food Science, University of Maryland, College Park, Maryland 20742 (Y.L.); Instrumentation and Sensing Laboratory, Henry A. Wallace Beltsville Agricultural Research Center, USDA, Building 303, BARC-East, 10300 Baltimore Avenue, Beltsville, Maryland 20705 (Y.-R.C., K.C.); and Food Technology and Safety Laboratory, Henry A. Wallace Beltsville Agricultural Research Center, USDA, Building 201, BARC-East, 10300 Baltimore Avenue, Beltsville, Maryland 20705 (X.N.)

Surface-enhanced Raman (SERS) spectra of various batches of bacteria adsorbed on silver colloidal nanoparticles were collected to explore the potential of the SERS technique for rapid and routine identification of *E. coli* and *L. monocytogenes* cultures. Relative standard deviation (RSD) of SERS spectra from silver colloidal suspensions and ratios of SERS peaks from small molecules (K_3PO_4) were used to evaluate the reproducibility, stability, and binding effectiveness of citrate-reduced silver colloids over batch and storage processes. The results suggested consistent reproducibility of silver colloids over batch process and also stability and consistent binding effectiveness over an eight-week storage period. A variety of mixtures of *E. coli*/*L. monocytogenes* cultures with different colloidal batches revealed that, despite large variations in relative intensities and positions of SERS active bands, characteristic and unique bands at 712 and 390 cm^{-1} were consistently observed and were the strongest in *E. coli* and *L. monocytogenes* cultures, respectively. Two specific bands were used to develop simple algorithms in the evaluation of binding effectiveness of silver colloids over storage and further to identify *E. coli* and *L. monocytogenes* cultures with a 100% success. A single spectrum acquisition took 5~6 min, and a minimum of 25 μL silver colloid was directly mixed with 25 μL volume of incubated bacterial culture. The short acquisition time and small volume of incubated bacterial culture make silver colloidal nanoparticle based SERS spectroscopy ideal for potential use in the routine and rapid screening of *E. coli* and *L. monocytogenes* cultures on large scales. This is the first report of the development of simple and universal algorithms for bacterial identification from the respective exclusive SERS peaks.

Index Headings: ***E. coli* bacteria; *L. monocytogenes* bacteria; Surface-enhanced Raman spectroscopy; SERS; Silver colloid nanoparticles; Algorithm; Bacterial identification; Safety.**

INTRODUCTION

Rapid, accurate, and preferably routine methods for the identification of food-borne bacteria are increasingly important because of not only the threat of bio-/agro-terrorism but also due to public health concern and economic loss resulting from unexpected food-borne outbreaks, such as *E. coli* contaminated spinach in September 2006[1] and *L. monocytogenes* tainted ham/turkey products in November 2006.[2] The traditional techniques developed since the 1980s are time-consuming, requiring 5–7 days, and are not sufficiently rapid to assure the safety of ready-to-eat food products.[3] Antibody-/nucleic acid probes based on system and amplification-based methods such as, most notably, polymerase chain reaction (PCR), have been developed as viable tools to detect bacteria.[4] However, these assays have encountered two major problems: false negatives/false positives identification and speed (>50 min).[4] More recently, biosensors have been developed for rapid and specific detection of bacteria at low levels on the basis of sandwich immunoassays involving a capture antibody and a detection (label) antibody.[5,6] These methods need to select optimal capture and detection antibodies, to wash out extra antibodies, and to allow some time (>30 min) for the immobilization of antibodies, indicating that they are multi-step procedures requiring chemical reagents, are labor intensive, and are prone to operator-to-operator variation.

Rapid microbial detection requires minimal sample preparation (e.g., to avoid the centrifugation/isolation/drying/washing process), permits routine analysis of a large number of samples with low reagent costs, and should be easy to operate. To limit the probability of bacterial cross-contamination, reducing bacterial exposure to the environment during the procedure and data accumulation is also desirable. The Raman technique is an alternative approach; not only has it been used to obtain highly structured information on bacteria,[7,8] even at the single bacterial cell level,[9] but it also lacks interference from water.

Generally, the Raman effect is very weak, due to its small scattering cross-section (only ~1 in 10^8 incident photos). However, it can be greatly enhanced by 10^3- to 10^{15}-fold by the surface-enhanced Raman scattering (SERS) method, if the analyte is attached (adsorbed) to or in close proximity to a specially prepared surface of noble metals such Au and Ag.[10,11] To better utilize the great potential signal enhancement of SERS, a number of different types of Au and Ag substrates have been developed, in the forms of metal colloids, roughened electrodes, and vacuum deposited metal/nanoparticle island films.[10–19] Among them, metal colloids typically provide the greatest SERS enhancement, and in some cases, these colloids have proven to be capable of trace component/single-molecule detection. Apparently, however, metal colloidal substrates have both reproducibility and stability concerns, as colloid particles might vary from batch to batch and tend to aggregate and to precipitate in solutions over time.[16,20]

Surface-enhanced Raman spectroscopic studies of bacteria adsorbed on fresh borohydride-reduced or citrate-reduced silver colloids have been reported, and the results reveal the potential of SERS in the fingerprinting characterization of bacterial structures.[16–19] However, these studies neither revealed unique SERS peaks for specific bacterial identification nor examined the effects of chemical components from growth media and/or metabolic byproducts on SERS spectra of diluted bacterial suspensions and bacterial biomass. Although different bacteria could be clearly distinguished with multivariate

Received 5 January 2007; accepted 16 May 2007.
* Author to whom correspondence should be sent. E-mail: yud-ren.chen@ars.usda.gov.

0003-7028/07/6108-0824$2.00/0

statistical techniques such as discriminant function analysis (DFA) and hierarchical cluster analysis (HCA), the chemometric models were developed from only one of three batches of colloidal silver solutions.[16] Probably, this indicates the challenge of applying multivariate data analysis to SERS spectra and the difficulty of producing repeatable SERS spectra from one batch of silver colloid to another.

The objectives of this study are: (1) to prepare citrate-reduced silver colloids and to evaluate both their reproducibility over batches and their stability over storage periods, (2) to assess the binding effectiveness of silver colloidal nanoparticles by using tripotassium phosphate (K_3PO_4), a small molecule, as the analyte, (3) to explore characteristic SERS bands of *E. coli* and *L. monocytogenes* cultures, and (4) to develop simple and universal algorithms for bacterial identification from their respective unique SERS bands. The ultimate goal is to develop the SERS technique for rapid, accurate, and routine detection of *E. coli* and *L. monocytogenes* for public safety and security. In addition, the use of Fourier transform (FT) methodology and a 1064 nm excitation laser in the near-infrared (NIR) region provides precise wavenumber measurement and good-quality SERS spectra by reducing the interference from fluorescence and photodecomposition.[21,22]

EXPERIMENTAL

Chemical Reagents and Glass Tubes. Chemical reagents (silver nitrate, >99%; trisodium citrate, >99%; tripotassium phosphate, >98%; dipotassium hydrogen phosphate, >98%; and glucose, >99.5%) and Trypic Soy Broth (pancreatic digest of casein : papain digest of soyabean : sodium chloride : dipotassium hydrogen phosphate : glucose monohydrate = 17 : 3 : 5 : 2.5 : 2.5) were purchased from Sigma-Aldrich (St. Louis, MO) and Becton, Dickinson and Company (Sparks, MD), respectively, and used without further purification. Disposable glass tubes (6 mm outside diameter × 50 mm length) were supplied by Fisher Scientific (Suwanee, GA).

Silver Colloid Preparation. During a six-month period, seven batches of citrate-reduced silver colloidal suspensions were prepared by a modified Lee and Meisel procedure.[23] Briefly, a clean 250 mL beaker containing 100 mL of distilled/deionized water and a magnetic stirring bar was placed on a stirrer hot plate and the beaker opening was covered with aluminum foil to minimize the loss of water. It was heated to approximately 45 °C, at which point 18 mg of silver nitrate was added. With further heating and stirring, the solution was brought to the boiling point and 2 mL of 1% (w/v) trisodium citrate was introduced. The solutions were boiled for ~15 min with continuous stirring, allowing sufficient time for formation of silver colloidal nanoparticles. These were indicated by the gradual color change from a colorless solution to a gray/green solution approximately 7 min after addition of the trisodium citrate. The beaker was taken off the heat and cooled to and kept at room temperature.

Bacterial Culture Preparation. Over 14 batches of *Escherichia coli* strains (*E. coli* ATCC 25922) and *Listeria monocytogenes* strains (*L. monocytogenes* ATCC 13932) were incubated overnight in Trypic Soy Broth (TSB) growth media at 37 °C and 35 °C, respectively, for approximately 17–20 hours without agitation over a span of six months. This growth procedure routinely yielded a culture containing ~10^9 colony forming units (CFU)/mL of each respective bacterium at the stationary phase. Before the SERS experiment, bacterial species were re-confirmed. TSB media was used because it was the easiest to prepare and had a wide application base.[24]

Surface-Enhanced Raman Spectra. The SERS spectra were collected on an FT-Raman module for the Nicolet 670 FT-IR bench (Madison, WI) using a DTGS KBr detector and XT-KBr beamsplitter. The 6 × 50 mm (outer diameter × length) glass tube containing the analyte–silver colloid mixture was illuminated using the Nd:YAG excitation laser operating at 1064 nm. Raman scatter was accumulated using the 180° reflective mode with 1 W of laser power at the mid-portion of the mixture and 256 scans at 8 cm^{-1} resolution. All spectra were transformed into .spc files (Grams file format) and then were smoothed with a second-order polynomial Savitzky–Golay function with 11 points by use of Grams/32 software (Version 7.0, Galactic Industries Corp., Salem, NH). The data set was loaded into Microsoft Excel 2000 to execute simple algorithm analysis.

Three types of SERS measurements were performed. First, 50 μL of different silver colloidal batches in both a fresh and an aging state were introduced into glass tubes to evaluate their reproducibility and stability. Second, 40 μL of an aqueous K_3PO_4 solution was added to the same volume of silver colloids to examine the binding effectiveness of silver nanoparticles. Third, *E. coli* and *L. monocytogenes* suspensions were mixed with silver colloids at a volume ratio of 1:1 (40 μL/40 μL) to uncover the respective bacterial characteristic bands. For one bacterial or K_3PO_4 solution against one batch colloidal solution, two measurements were taken. Immediately after mixing the two solutions, the glass tubes were vigorously shaken five times and then left untouched for 10 min before the subsequent SERS measurements were taken. Although it is possible that the volume ratio of 1:1 and the 10 min binding interval might not be the optimum parameters, our pre-experimental tests from a number of different volume ratios and a variety of time evolutions after the mixing suggested that the use of a 1:1 volume ratio and 10 min binding time could yield good quality and acceptable SERS spectra because silver particles were observed to precipitate out gradually in cultures 25–30 min following the mixing procedure.

RESULTS AND DISCUSSION

Reproducibility and Stability of Silver Colloids. One of the major concerns in SERS studies is to prepare reproducible silver colloids with the batch process, as the fabrication procedure is sensitive to many factors, such as temperature,[25] period of mixing,[25] and rate of addition of reagents.[26] Semiautomatic flow systems have been developed and might provide a solution.[20]

Figure 1 shows the average (middle spectrum) ± standard deviation (SD, upper spectrum and lower spectrum) spectra of SERS signals from seven fresh silver colloidal suspensions prepared with the batch process in the 1700–100 cm^{-1} region. Before computing the mean, seven SERS spectra were normalized at the 215 cm^{-1} peak by scaling its maximum intensity to be 1. It can be seen that, besides the 215 cm^{-1} band, there are no other significant SERS peaks arising from decomposed chemical residuals and water in the silver colloids. The 215 cm^{-1} band might be due to colloidal scattering and be associated with size, aggregation, and size distributions of silver nanoparticles.

The plot of relative standard deviation (RSD, ratio of SD against intensity in the average SERS spectrum) in Fig. 2a

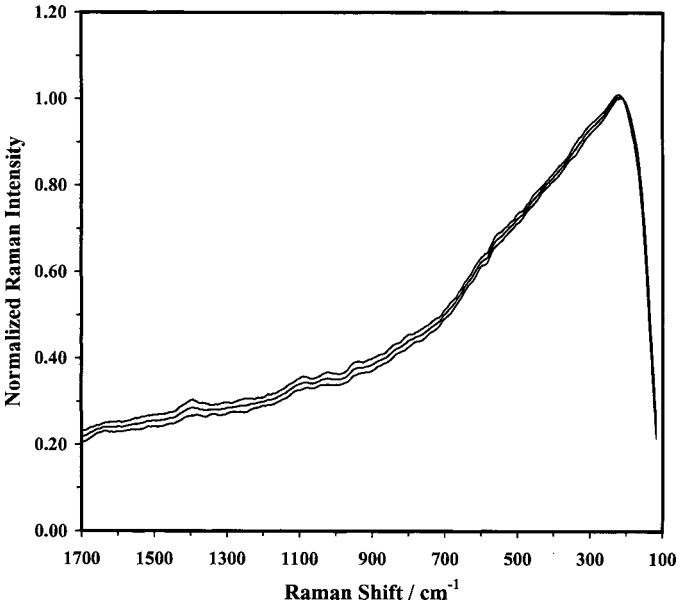

FIG. 1. Average SERS (***middle***) ± standard deviation (SD, ***upper*** and ***lower***) spectra of seven fresh silver colloidal suspensions prepared with a batch process.

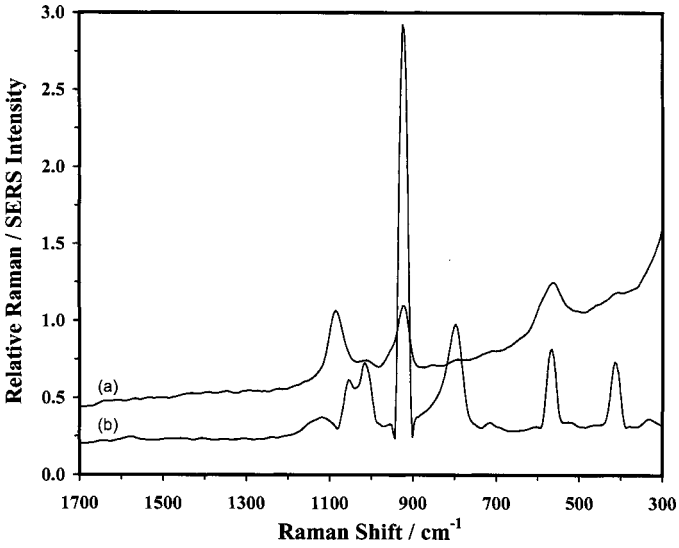

FIG. 3. (***a***) SERS spectrum of a K_3PO_4 aqueous solution (final concentration of 5.0×10^{-3} M); (***b***) FT-Raman spectrum of K_3PO_4 in the solid state (intensity was reduced by 50% for clarity).

suggests that there is less variation (<5%) in the 1100–150 cm^{-1} region than in the 1700–1100 cm^{-1} region. This could indicate the consistency and reproducibility of size, aggregation, and size distributions of silver colloidal nanoparticles prepared with the batch process.

Besides the 215 cm^{-1} peak, there are no additional SERS peaks observed in the 1700–150 cm^{-1} region for the silver colloids during an eight-week storage period at room temperature. This suggests the stability of the silver colloidal suspensions and is consistent with other reports.[26,27] Similarly, normalized SERS spectra were obtained and RSDs are plotted in Fig. 2b. Less than 5% variation below 1100 cm^{-1} indicates the stability of silver colloidal nanoparticles over storage.

Binding Effectiveness of Silver Colloidal Nanoparticles with K_3PO_4. In addition to measuring the ultraviolet (UV)-visible and SERS spectra of silver colloids in the pure state for the examination of reproducibility and stability, a model compound with characteristic bands has been introduced into the colloidal solutions.[20] For example, the dye 3,5-dimethoxy-4-(5'azobenzotriazole) phenylamine was used to compare the reproducibility of silver colloids prepared using two methods, the flow system and the batch process.[20] In this study, K_3PO_4 was selected as an analyte because it is much smaller than the silver colloidal nanoparticles, has a simple structure, and has characteristic P–O vibrations.

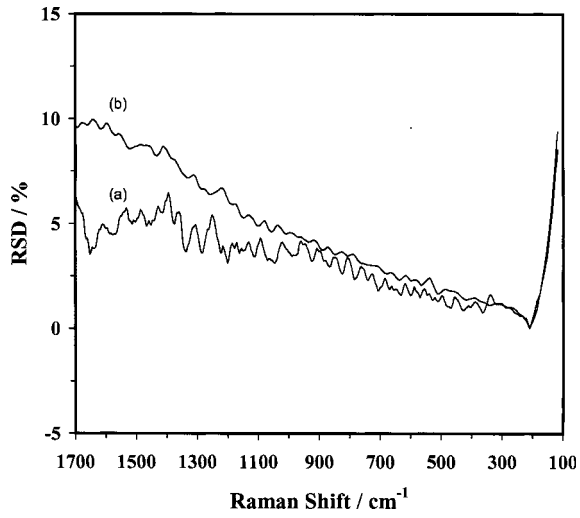

FIG. 2. Relative standard deviation (RSD) of SERS spectra for silver colloids (***a***) over the batch process and (***b***) over the storage period.

Figure 3a shows the SERS spectrum of an aqueous K_3PO_4 solution at a final concentration of 5×10^{-3} M in the region of 1700–300 cm^{-1}, excluding the peak of silver colloids below 300 cm^{-1}. Clearly, there are three intense SERS-active bands at 1086, 922, and 564 cm^{-1}, and at least three very weak ones near 1020, 730, and 415 cm^{-1}. As a comparison, the FT-Raman spectrum of K_3PO_4 in the solid state is presented in Fig. 3b, and it is dominated by a very strong band near 922 cm^{-1}, which arises from the symmetric P–O stretching mode (ν_1), and other Raman-active bands at approximately 1050 and 1012 cm^{-1} (ν_3, antisymmetric P–O stretching mode), 792 cm^{-1} (unknown mode), 564 cm^{-1} (ν_4, P–O rocking mode), and 415 cm^{-1} (ν_2, P–O twisting mode).[28–30] Therefore, strong SERS-active bands at 1086, 922, and 564 cm^{-1} can be assigned to the ν_3, ν_1, and ν_4 of modes of the phosphate group, respectively. Notably, ν_1 and ν_4 SERS-active bands appear at exactly the same wavelengths as Raman-active ones, and the SERS-active ν_3 band up-shifts from 1050/1020 cm^{-1} in the Raman spectrum to 1086 cm^{-1}. Both the appearance of the ν_1 and ν_4 bands and the shift of the ν_3 band in the SERS spectrum indicate that the ν_1 and ν_4 bands are not influenced by the hydrogen bonding because the K_3PO_4 molecule exists in a monomeric form in such a diluted solution. Consequently, the intense and separated ν_1 band could be used to evaluate the binding effectiveness of silver colloidal nanoparticles.

Figure 4 plots the storage-time-dependent binding effectiveness of silver colloidal nanoparticles with K_3PO_4 solutions of 1.0×10^{-2} M, by using the ratio of the SERS intensity at 922 cm^{-1} against the intensity at 850 cm^{-1}, at which wavelength no

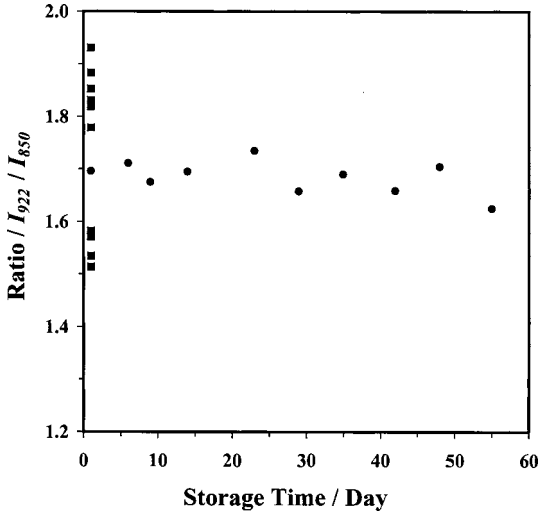

FIG. 4. Storage-time-dependent binding effectiveness of silver colloidal nanoparticles with K_3PO_4 aqueous solution (final concentration: 5.0×10^{-3} M) by using the I_{922}/I_{850} values (•). I_{922}/I_{850} ratios (■) from both seven fresh colloidal batches and seven repeated measurements of one fresh colloidal batch were inserted at the far left for comparison.

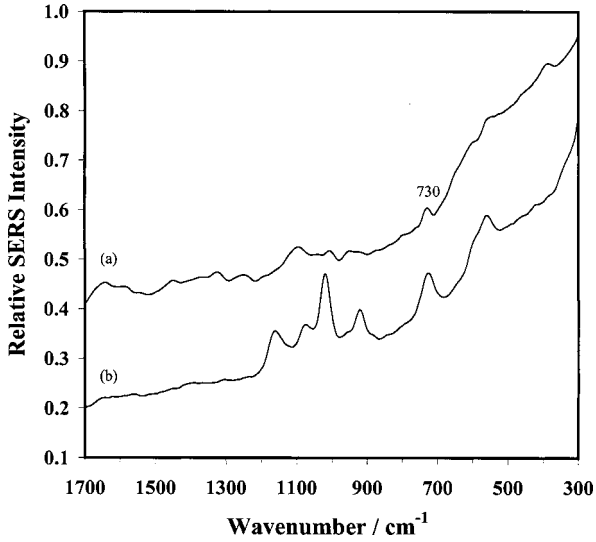

FIG. 5. SERS spectra of (***a***) TSB growth medium and (***b***) an aqueous K_2HPO_4 solution (final concentration: 1.25 g/L or 7×10^{-3} M). SERS intensity of K_2HPO_4 was reduced by 25% for clarity.

SERS peaks were observed. The value of I_{922}/I_{850} (shown as solid circles) tends to decrease slightly but is relatively consistent, suggesting that the binding capability of silver colloidal nanoparticles with K_3PO_4, a much smaller molecule, is obviously unaffected during the eight-week storage period. Meanwhile, the I_{922}/I_{850} values (shown as solid squares) from either seven fresh batches (Day 1) or seven replicate measurements of one fresh batch were inserted at the far left in Fig. 4. Apparently, variations of binding effectiveness of silver colloidal nanoparticles over batches even within one batch are greater than variations of colloids over the storage period, with RSDs of 8.7% and 1.8% for the batch process and for the storage process, respectively. This result is very close to the best reported RSD of 6.6% between the citrate-stabilized borohydride-reduced silver colloids prepared using the flow system,[20] indicating that using a batch process can produce reproducible citrate-reduced silver colloidal nanoparticles.

Surface-Enhanced Raman Spectroscopic Characteristics of Growth Media. The TSB growth media, composed of a mixture of organic and inorganic nutrients, shows several broad and weak SERS bands (Fig. 5a). While there is the possibility to obtain chemical information from a SERS spectrum, it is difficult to interpret it because there could be any number of SERS-active modes in a biochemically complex growth medium. To be particularly noted is the band near 730 cm^{-1}, which has been assigned to a vibrational mode of the glycosidic ring in glucose.[16] The SERS spectrum of glucose at a concentration of 2.5 g in 1000 mL distilled water in this laboratory did not exhibit the 730 cm^{-1} band. However, dipotassium hydrogen phosphate (K_2HPO_4) shows the 730 cm^{-1} SERS peak as shown in Fig. 5b, indicating that the 730 cm^{-1} SERS band could be attributed to the symmetric O–P–O vibrational mode of the phosphate group.[31] The reason that other SERS-active phosphate bands at 1160, 1070, 1012, 922, and 564 cm^{-1} could not be observed clearly in Fig. 5a might likely be physical, chemical, and structural changes of the phosphate group in the TSB solution because of multi-component interactions through a number of factors such as hydrogen bonds and van Der Waals forces. Meanwhile, the ν_1 and ν_4 absorption wavelengths in K_2HPO_4 (Fig. 5b) are identical to those of K_3PO_4 in Fig. 3b, again suggesting that the ν_1 and ν_4 bands arise from P–O vibrations and are independent of structural differences between them.

Surface-Enhanced Raman Spectroscopic Characteristics of *E. coli* Cultures. Figure 6 shows typical SERS spectra from mixtures of different batches of *E. coli* cultures and silver colloidal suspensions, in which Figs. 6a and 6b compare the spectra of the same batch of *E. coli* in two batches of colloids, while Figs. 6c and 6d present the spectra of two batches of *E. coli* in one batch of silver colloid. As a comparison, the FT-Raman spectrum of the *E. coli* culture is given and marked as

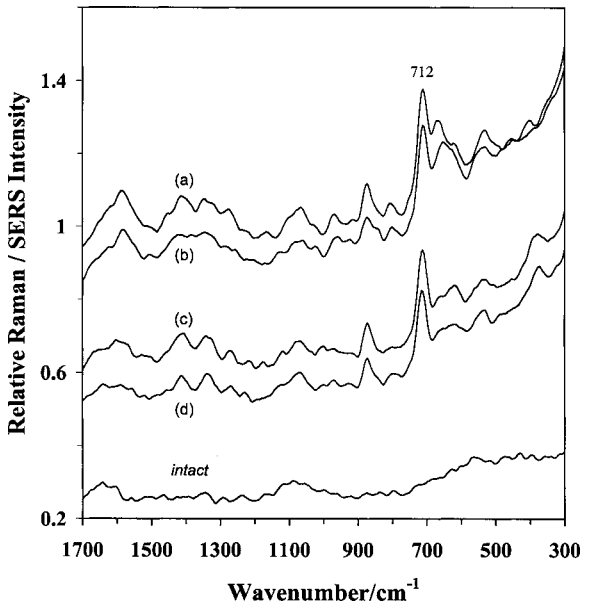

FIG. 6. Representative SERS spectra of *E. coli* cultures; (***a***) and (***b***) represent the same batch of *E. coli* in two batches of silver colloids, while (***c***) and (***d***) compare two batches of *E. coli* in one batch of silver colloid. As a comparison, an FT-Raman spectrum of *E. coli* culture, labeled as ***intact***, is provided.

TABLE I. Assignment of SERS peaks for *E. coli* culture, *L. monocytogenes* culture, TSB, K_3PO_4, and K_2HPO_4. (Notation: m = medium, s = strong, vs = very strong, vw = very weak, w = weak.)

E. coli	*L. monocytogenes*	TSB	K_3PO_4	K_2HPO_4	Tentative peak assignment[8,16–18,32]
1640 (w)	1640 (m)	1640 (m)			Amide I, water
1585 (s)	1585 (m)	1580 (w)			C=C (lipid)
	1453 (m)	1440 (w)			CH_2 bend
1411 (s)					COO^- symmetric stretch
1342 (s)					CH bend (protein)
1273 (m)		1240 (w)			amide III
1120 (w)				1160 (m)	ν_3 of phosphate
	1085 (m)	1080 (s)	1086 (s)		ν_3 of phosphate
1070 (s)				1070 (m)	ν_3 of phosphate
			1020 (vw)	1012 (s)	ν_3 of phosphate
	1006 (s)				ν_3 of phosphate
968 (m)					C–N stretch
		922 (vw)	922 (s)	922 (m)	ν_1 of phosphate
873 (s)					
802 (w)					C–N stretch
712 (vs)		730 (m)	730 (vw)	730 (m)	POP symmetric stretch
665 (s)					COO^- bend
			564 (s)	564 (m)	ν_4 of phosphate
540 (s)		545 (w)			ν_4 of phosphate
			415 (vw)	415 (vw)	ν_2 of phosphate
	390 (vs)				ν_2 of phosphate
375 (m)		375 (w)			ν_2 of phosphate

intact in Fig. 6, and it does not show any bands except water. As expected, there are large variations in both the relative intensity and the position of SERS-active bands from one *E. coli* solution to another because of subtle changes among silver colloidal batches and unpredicted metabolic processes between bacterial batches. Because *E. coli* cultures consist of numerous species, which pre-existed in growth media and were produced as the byproducts during the bacterial growth, clear understanding of the origins of SERS-active bands is not straightforward. However, tentative band assignments could be made by referring to other SERS and Raman studies of *E. coli*, and these are summarized in Table I.[8,16–18] Notably, There are great discrepancies in the relative SERS intensities between this study and others,[16–18] probably because of different growth media (TSB versus Luria broth),[17,18] different ratios of bacteria/silver colloidal suspensions (1:1 versus 1:50),[7] different treatment of incubated bacterial suspensions (intact versus diluted or centrifuged/washed),[16,17] different presentation of bacterial/silver colloid mixtures (in solutions versus dried on CaF_2 disks),[16] and different excitation lasers (1064 nm versus 514.5 nm[17,18] and 785 nm[16]). In addition, the appearance of SERS peaks might differ from silver to gold colloidal solution.[32]

Despite the fluctuations in relative intensity and position of the SERS bands over both *E. coli* and silver colloidal batches, these SERS spectra do show several common bands. Among them, the 712 cm^{-1} band is quite interesting because it always appears and is the strongest and sharpest of the bands. This band might result from the shift of the 730 cm^{-1} peak due to the conditional change from TSB growth media to incubated bacterial cultures. To unravel the persistence of the 712 cm^{-1} band, both supernatants from *E. coli* suspensions and diluted *E. coli* cultures, by adding either growth medium or silver colloid, were prepared, and the resulting SERS spectra consistently exhibited a dominant peak at 712 cm^{-1}. Therefore, the 712 cm^{-1} band could potentially be used to identify *E. coli* cultures.

As *E. coli* cultures had a pH of approximately 6.0 and consisted of chemical and biological species in varying sizes, they might have different binding effectiveness with silver colloidal nanoparticles. Figure 7 depicts the storage-time-dependent binding effectiveness of silver colloidal nanoparticles with *E. coli* suspensions (indicated by solid circles) by using the ratio of the SERS intensity at 712 cm^{-1} against the intensity at 730 cm^{-1}. It suggests that the binding capability between *E. coli* suspensions and silver nanoparticles is nearly unchanged with 8-week storage of colloids. A major reason might be the low pH in incubated *E. coli* cultures, as acidic conditions could increase the binding affinity of the amino acid group to colloidal particles and result in more intense SERS bands.[33] On the other hand, such acidic cultures destroyed the stability of silver colloids and caused the colloids to be short-lived, as evidence from the precipitation of silver particles in

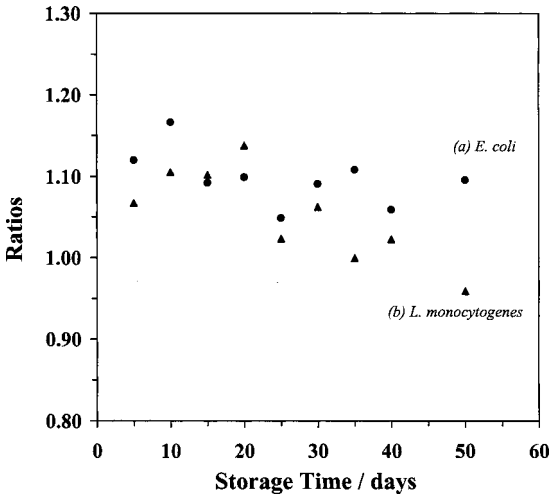

FIG. 7. Storage-time-dependent binding effectiveness of silver colloidal nanoparticles with (***a***) *E. coli* and (***b***) *L. monocytogenes* cultures.

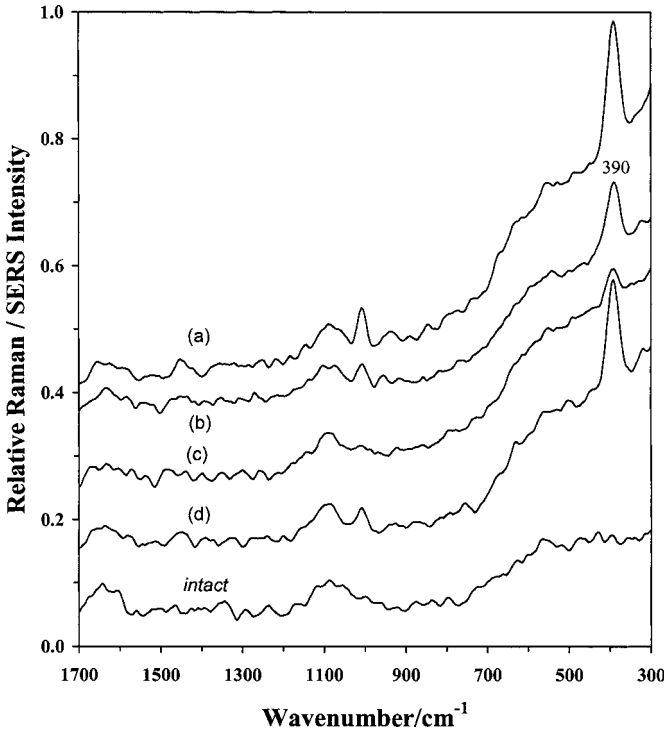

FIG. 8. Representative SERS spectra of *L. monocytogenes* cultures; (***a***) and (***b***) represent the same batch of *L. monocytogenes* in two batches of silver colloids, while (***c***) and (***d***) compare two batches of *L. monocytogenes* in one batch of silver colloid. As a comparison, an FT-Raman spectrum of *L. monocytogenes* culture, labeled as ***intact***, is provided.

the bottom of the tube around 25–30 min later and the lack of SERS peaks after 2 h.

Surface-Enhanced Raman Characteristics of *L. monocytogenes* Cultures. The Fourier transform Raman spectrum of an *L. monocytogenes* culture and representative SERS spectra of three *L. monocytogenes* batches in different silver colloidal suspensions are shown in Fig. 8, in which Figs. 8a and 8b compare the spectra of one *L. monocytogenes* culture in two colloidal batches, whereas Figs. 8c and 8d compare those of two *L. monocytogenes* batches in one colloidal suspension. Similar to the observation in Fig. 6, there are large differences in both the relative intensity and the position of the SERS-active bands within *L. monocytogenes* cultures, and their characteristic bands are also listed in Table I. Close examination of the SERS spectra yields a 390 cm^{-1} band that is common, the strongest, and the best separated, indicating that this 390 cm^{-1} band might be useful for the identification of *L. monocytogenes* suspensions.

The most striking difference between the SERS spectra of *E. coli* and *L. monocytogenes* cultures is the appearance of much more prominent SERS peaks in the *E. coli* suspensions. Such distinctions could be a reflection of the genetic, structural, or metabolic differences between two very distinctive microorganisms: *E. coli* is in the *Enterobacteriacae* family and *L. monocytogenes* is in the *Listeriaceae* family. Therefore, intense and well-isolated 712 and 390 cm^{-1} SERS peaks could be used to discriminate *E. coli* suspensions from *L. monocytogenes* suspensions. Undoubtedly, the use of different growth parameters could result in characteristic SERS peaks at wavelengths other than those at 712 and 390 cm^{-1} observed here.

The binding capability between *L. monocytogenes* cultures and silver colloidal suspensions, given by the ratio of the SERS intensity at 390 cm^{-1} against the intensity at 352 cm^{-1}, shown in Fig. 7b, is effective during the first 30-day storage period and then decreases afterwards. Meanwhile, the ratio of I_{390}/I_{352} approaches 1 after 35–40 days of storage, suggesting that silver colloidal suspensions at this stage could hardly be used for identifying *L. monocytogenes* cultures.

Comparison of the ratios between *E. coli* and *L. monocytogenes* cultures, together with those for K_3PO_4 in Fig. 4, indicates that the binding effectiveness of silver nanoparticles with K_3PO_4 (molecule is much smaller than the silver nanoparticles) is larger than that with a complex bacterial suspension (bacterial cells are much larger than the colloidal nanoparticles). Probably, the co-existence of numerous species with varying molecular sizes in cultures might alter the physical, chemical, and surface structure of silver colloidal nanoparticles and lead to their reduced binding effectiveness.

Although silver colloids were stable for several months, their storage-time-dependent binding capability depends on the type of analyte. For example, adsorption of K_3PO_4 and *E. coli* solutions on silver nanoparticles is relatively consistent while that of *L. monocytogenes* decreases obviously after 35–40 days. Noticeably, nearly all of the ratios are greater than 1, suggesting that the characteristic bands are discernable and have the power to identify individual analytes, while irregular up-and-down ratios with storage time indicate that, besides the volume ratio of analyte against colloidal solution and waiting time after mixing of two suspensions, variations within solutions and colloidal batches as well as data accumulation time might produce unpredictable SERS intensities of analyte adsorbed on silver nanoparticles.

Identification of *E. coli* and *L. monocytogenes* Cultures from Simple Algorithms. It is of interest to examine whether *E. coli* and *L. monocytogenes* cultures could be identified from simple intensity ratios. As discussed above and reported by others,[16] SERS bands vary greatly even for one analyte in different silver colloidal batches. Therefore, in this work, one bacterial culture was mixed with at least two batches of silver colloidal suspensions that were stored for different periods, and the SERS data only from colloidal solutions stored less than 40 days were used. Figure 9 shows the ratio of I_{712}/I_{730} (horizontal) against the ratio of I_{390}/I_{352} for 18 batches of *E. coli* cultures, 14 batches of *L. monocytogenes* cultures, and a number of batches of TSB growth media and silver colloidal suspensions that both were stored for various periods.

Figure 9 reveals an excellent separation and indicates that the *E. coli* and *L. monocytogenes* cultures can be correctly discriminated from each other and also from TSB growth media and silver colloidal suspensions, by the ratio values of I_{712}/I_{730} greater than 1.04 and the ratio values of I_{390}/I_{352} greater than 1.03, respectively. *E. coli* and *L. monocytogenes* cultures, as well as growth media, display more scatter distribution than silver colloids, probably due to a number of factors, such as the variation of chemical components and heterogeneities over batches of bacterial cultures and colloidal suspensions, time after mixing bacteria and colloids, and bacterial preparation. Meanwhile, close disposition of silver colloids suggests reproducibility, consistency, and stability over batch and storage. Notably, the classification model is based upon SERS spectra acquired from different colloidal batches stored for different lengths of time.

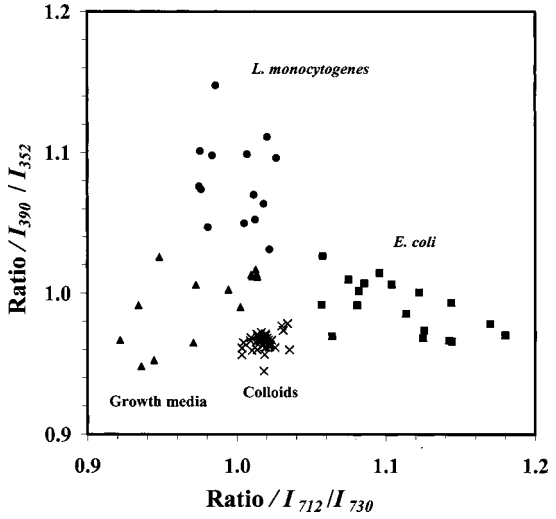

FIG. 9. Plot of the ratio of I_{712}/I_{730} (horizontal) versus one of I_{390}/I_{352} (vertical) for *E. coli* cultures (■), *L. monocytogenes* cultures (•), TSB growth media (▲), and silver colloids (×). Each point was the average of at least four SERS measurements of *E. coli*, *L. monocytogenes*, and growth media in two silver colloidal batches that were stored for a period of less than 40 days.

Although multivariate data analysis of SERS spectra has been attempted to discriminate different bacteria, SERS data from only one batch of colloid were used.[16] Clearly, this is impractical and might result in the loss of some information. Furthermore, preprocessing of SERS spectra, such as subtracting a linearly increasing baseline[16] and normalizing the spectra at the 1635 cm^{-1} water peak,[17] are time consuming and subjective. Consequently, development of ratio algorithms utilizing the unique SERS bands directly in the current work is simple and can be universally applied for fast, accurate, and routine screening of *E. coli* and *L. monocytogenes* cultures on a variety of silver colloidal suspensions over batches and storage periods.

CONCLUSION

This study demonstrates the potential of the SERS technique for rapid and routine identification of *E. coli* and *L. monocytogenes* cultures adsorbed on silver colloidal nanoparticles. To extract useful information from the poorly reproducible SERS signal of biological analytes, spectra of various mixed batches of *E. coli* and *L. monocytogenes* cultures as well as growth media with different colloidal batches were examined. Particularly, characteristic bands at 712 and 390 cm^{-1} consistently appeared and had the strongest intensity, and were identified from *E. coli* and *L. monocytogenes* cultures, respectively. These two unique bands were then used to develop simple algorithms in the assessment of the binding effectiveness of silver colloidal nanoparticles over storage time and further to identify *E. coli* and *L. monocytogenes* cultures with 100% success. This is the first report of characteristic SERS bands of *E. coli* and *L. monocytogenes* suspensions and the development of simple and universal algorithms for bacterial detection from the respective exclusive SERS peaks.

To assess the reproducibility and stability of citrate-reduced silver colloids over batch process and over storage period, as well as their binding effectiveness, the relative standard deviation (RSD) of normalized SERS spectra of silver colloid suspensions and the ratio of the SERS-active P–O band at 922 cm^{-1} in K_3PO_4 aqueous solutions were used. The results revealed a less than 5% variation of RSD in the 1100–150 cm^{-1} region for silver colloids over both batch process and storage period and a greater variation of binding effectiveness within colloidal batches than within colloidal storage periods. However, the RSD of 8.7% from the I_{922}/I_{850} ratios of K_3PO_4 solutions against different colloidal batches was very close to the best reported RSD value of 6.6% using the flow system,[20] suggesting that batch process can produce reproducible citrate-reduced silver colloidal nanoparticles.

Binding effectiveness of silver colloidal suspensions with small molecules (K_3PO_4) was greater than that of the *E. coli* and *L. monocytogenes* matrix. Although silver colloidal nanoparticles were stable for several months, their storage-time-dependent binding effectiveness suggested that adsorption of *E. coli* and K_3PO_4 is nearly consistent over the eight-week storage period, whereas that of *L. monocytogenes* decreases apparently after 35–40 days.

From a practical viewpoint, this study provides sufficient definitions and suggests simple procedures to fabricate silver colloids, to sample bacterial cultures, and to analyze SERS spectra. Notably, this method requires no purification/separation/drying/washing process, uses as few as 25 μL colloidal or bacterial suspensions, and is fast in data collection and species identification. Hence, the SERS technique can be used for rapid, specific, and routine screening of bacteria in ready-to-eat food products, in manufacturing process control, and in monitoring of cleaning and hygiene practices.

ACKNOWLEDGMENTS

Mention of a product or specific equipment does not constitute a guarantee or warranty by the U.S. Department of Agriculture and does not imply its approval to the exclusion of other products that may also be suitable.

The authors wish to express their sincere thanks to Ms. Jessica Delgado of ARS/USDA, Beltsville, for culturing bacterial suspensions.

1. FDA, http://www.fda.gov/bbs/topics/NEWS/2006/NEW01451.html (accessed November 27, 2006).
2. USDA, http://www.fsis.usda.gov/News_&_Events/Recall_033_2006_Release/index.asp (accessed November 27, 2006).
3. C. W. Donnelly, in *Listeria, Listeriosis, and Food Safety*, T. Ryser and E. H. Marth, Eds. Marcel Dekker, New York, 1999), 2nd ed., p. 225.
4. C. A. Batt, in *Listeria, Listeriosis, and Food Safety*, T. Ryser and E. H. Marth, Eds. (Marcel Dekker, New York, 1999), 2nd ed., p. 261.
5. T. Geng, J. Uknalis, S.-I. Tu, and A. K. Bhunia, Sensors **6,** 796 (2006).
6. T. Geng, M. T. Morgan, and A. K. Bhunia, Appl. Environ. Microbiol. **70,** 6138 (2004).
7. W. H. Nelson, R. Manoharan, and J. F. Sperry, Appl. Spectrosc. Rev. **27,** 67 (1992).
8. Q. Wu, T. Hamilton, W. H. Nelson, S. Elliott, J. F. Sperry, and M. Wu, Anal. Chem. **73,** 3432 (2001).
9. T. A. Alexander, P. M. Pellegrion, and J. B. Gillespie, Appl. Spectrosc. **57,** 1340 (2003).
10. M. Moskovits, Rev. Mod. Phys. **57,** 783 (1985).
11. R. P. Van Duyne, in *Chemical and Biochemical Applications of Laser*, C. B. Moore, Ed. (Academic Press, New York, 1979), vol. IV, p. 101.
12. H. Li and B. M. Cullum, Appl. Spectrosc. **59,** 410 (2005).
13. J. C. Hoogvliet, M. Dijksma, B. Kamp, and W. P. van Bennekom, Anal. Chem. **72,** 2016 (2000).
14. L. A. Lyon, M. D. Musick, and M. J. Natan, Anal. Chem. **70,** 5177 (1998).
15. S. Nie and S. R. Emory, Science (Washington, D.C.) **275,** 1102 (1997).
16. R. M. Jarvis and R. Goodacre, Anal. Chem. **76,** 40 (2004).
17. A. Sengupta, M. L. Laucks, and E. J. Davis, Appl. Spectrosc. **59,** 1016 (2005).
18. M. L. Laucks, A. Sengupta, K. Junge, E. J. Davis, and B. D. Swanson, Appl. Spectrosc. **59,** 1222 (2005).
19. L. Zeiri, B. V. Bronk, Y. Shabtai, J. Czege, and S. Efrima, Colloids Surf. A **208,** 357 (2002).

20. R. Keir, D. Sadler, and W. E. Smith, Appl. Spectrosc. **56,** 551 (2002).
21. J. R. Ferraro and K. Nakamoto, *Introductory Raman Spectroscopy* (Academic Press, San Diego, 1994).
22. Y. Ozaki, "Raman Spectroscopy", in *Spectral Methods in Food Analysis,* M. M. Mossoba, Ed. (Marcel Dekker, New York, 1999), pp. 427–462.
23. P. C. Lee and D. Meisel, J. Phys. Chem. **86,** 3391 (1982).
24. M. N. Guerini, T. M. Arthur, S. D. Shackelford, and M. Koohmaraie, J. Food Protection **69,** 1007 (2006).
25. N. Shirtcliffe, U. Nickel, and S. Schneider, J. Colloid Interface Sci. **211,** 122 (1999).
26. C. H. Munro, W. E. Smith, M. Garner, J. Clarkson, and P. C. White, Langmuir **11,** 3712 (1995).
27. W. Ke, D. Zhou, J. Wu, and K. Ji, Appl. Spectrosc. **59,** 418 (2005).
28. E. J. Baran and K. H. Lii, Z. Naturforsch. **58,** 485 (2003).
29. J. Baran, T. Lis, and H. Ratajczak, J. Mol. Struct. **195,** 159 (1989).
30. H. Tsuda and J. Arends, J. Dent. Res. **72,** 1609 (1993).
31. Y. Guan, C. J. Wurrey, and G. J. Thomas, Biophys. J. **66,** 225 (1994).
32. W. R. Premasiri, D. T. Moir, M. S. Klempner, N. Krieger, G. Jones II, and L. D. Ziegler, J. Phys. Chem. B **109,** 312 (2005).
33. X. Dou, Y. M. Jung, H. Yamamoto, S. Doi, and Y. Ozaki, Appl. Spectrosc. **53,** 133 (1999).